

Three New Supercomputers to NSC



Kent-Roger Wistrand, Country Manager, HP, Bengt Persson director NSC and Jan Wallenberg, CEO, Go Virtual signs the contract.

Computational Fluid Dynamics

Professor Lars Davidson and his group at Chalmers works on method development for Computational Fluid Dynamics, CFD. NSC have provided extensive parallelization and optimization support of his code.

Read further on page 3

Three New Supercomputers to NSC

NSC has signed a contract with Go Virtual Nordic AB of delivery of three new computer systems from HP. The largest with a peak performance of 338 Teraflop.

Read further on page 6



NSC procures three new clusters

It is with great pleasure that NSC can announce that we have now ordered three new clusters – one for SNIC users, one for SMHI users and one for Saab users. The new cluster Triolith for SNIC users will make it possible to perform calculations and simulations at a new level. The cluster will have a theoretical peak performance of 338 TFlops/s making it the fastest supercomputer of Sweden. Triolith will be fully available for SNIC users by the end of 2012 and thereby be a worthy successor of Neolith with close

to 6 times increase of peak performance but looking at application performance we expect even greater increase. The system will be a powerful addition to the SNIC landscape of high performance computing, making NSC even better in serving our users' increased needs in all scientific branches, ranging from physics and chemistry to bioinformatics and other life sciences. NSC is now also procuring a new system for SMHI, providing increased computational capacity making it possible to improve weather forecasts even more in the future. Furthermore, we procure a cluster for Saab to serve their state-of-the-art computational needs. Technical details of the new clusters are presented in this issue.

For the SNAC application round this spring, you may have notice that a new and improved application system was introduced. The new system was jointly developed by NSC and C3SE in Gothenburg. The new system makes it easier for all users to apply for resources and more efficient to evaluate applications for the SNIC referees.

SNIC is from 2012 reformed as a distributed national research infrastructure, hosted by Uppsala University. A new board has recently been elected, and a new SNIC director is expected to start in June. More about this in next issue of NSC News.

Our e-science collaboration with PDC and the three major Stockholm universities is already successfully proceeding on its third year, and our SeRC annual meeting was held on 24–25 April in Stockholm. Participating SeRC staff gave a number of interesting scientific presentation and had an excellent opportunity to start new scientific collaborations.

Finally, we are happy that NSC continues to expand its staff, and we expect additional 8 new colleagues during this year. Now in March we welcomed Marvin Lie, who is presented in more detail in this issue.

BENGT PERSSON, NSC DIRECTOR

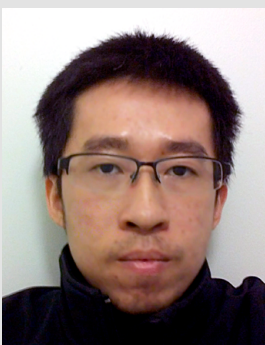
NSC is Expanding

Akademiska Hus is building a new computer room facility for NSC. The design and drawings are finalized and very soon the contracted work will commence. Initially there will be a computer room that can support three to four thousand servers but the building will have space to house a lot more computer capacity in the future.

Similar to the existing computer room, Hangaren, the new computer room will be connected to district cooling which Tekniska Verken in Linköping produce either by using outside air (during winter) or by waste incineration (during summer). To provide power and cooling to the new building, a new distribution central is built that will also strengthen the infrastructure on the entire LiU campus and in the surrounding area.

The new computer room will be ready in the beginning of 2013 and will enable NSC to deliver and support the growing needs of computing and storage capacity at academic institutions throughout Sweden as well as NSC partners.

NICLAS ANDERSSON, NSC



New staff member

I was kind of late into computers when it was a privilege to have one but not sort of compulsory like nowadays. My first computer was an IBM PC with an i80286 processor. Like everyone else I started by playing games and then learned program languages. Typing Tutor, Pinball Fantasy anyone? I also had fun with interrupts in MS DOS where a two bytes program actually can reboot the system. Over the years, I became more interested in trying out various MS Windows and open source software when OS running in real mode was practically dead. The experience with Linux is probably the one that got me into a system expert job in NSC.

MARVIN LIE

A Zonal LES/RANS Method Based on a

1 Introduction

Fluid flow problems are governed by the Navier-Stokes equations

$$\frac{\partial v_i}{\partial t} + \frac{\partial v_i v_j}{\partial x_j} = -\frac{1}{\rho} \frac{\partial p}{\partial x_i} + \nu \frac{\partial^2 v_i}{\partial x_j \partial x_j} \quad (1)$$

where v_i denotes the velocity vector, p is the pressure and ν and ρ are the viscosity and density of the fluid, respectively. In turbulent flow, the velocity and pressure are unsteady and v_i and p include all turbulent motions, often called eddies. The spatial scale of these eddies vary widely in magnitude where the largest eddies are proportional to the size of the largest physical length (for example the boundary layer thickness, δ , in case of a boundary layer). The smallest scales are related to the eddies where dissipation takes place, i.e. where the kinetic energy of the eddies is transformed into internal energy causing increased temperature. The ratio of the largest to the smallest eddies increases with Reynolds number, $Re = |v_i| \delta / \nu$, which means that the cell size in a computational mesh must be finer and finer for increasing Reynolds number. This has the unfortunate consequence – unless one is a fan of huge computer centers – that it is computationally extremely expensive to solve the Navier-Stokes equations for large Reynolds numbers.

1.1 Reynolds-Averaging Navier-Stokes equations: RANS

In order to be able to solve the Navier-Stokes equations with a reasonable computational cost, the velocity vector and the pressure are split into a time-averaged part (V_i and P) and a fluctuating part (v'_i and p'), i.e. $v_i = V_i + v'_i$, $p = P + p'$. The resulting equation is called the RANS (Reynolds-Averaging Navier-Stokes) equations

$$\frac{\partial V_i V_j}{\partial x_j} = -\frac{1}{\rho} \frac{\partial P}{\partial x_i} + \nu \frac{\partial^2 V_i}{\partial x_j \partial x_j} - \frac{\partial \overline{v'_i v'_j}}{\partial x_j} = -\frac{1}{\rho} \frac{\partial P}{\partial x_i} + \frac{\partial}{\partial x_j} \left((\nu + \nu_t) \frac{\partial V_i}{\partial x_j} \right) \quad (2)$$

The term in front of the second equal sign is called the Reynolds stress and it is unknown and must be modelled. All turbulent fluctuation are modelled with a turbulence model and the results when solving Eq. 2 are highly dependent on the accuracy of the turbulence model. On the right side of Eq. 2 the unknown Reynolds stresses are expressed by a turbulence model in which a new unknown variable is introduced which is called the turbulent viscosity, ν_t . The ratio of ν_t to ν may be of the order of 1000 or larger. In industry today, CFD (Computationally Fluid Dynamics) based on finite volume methods is used extensively to solve the RANS equations, Eq. 2.

1.2 Large Eddy Simulations: LES

A method more accurate than RANS is LES (Large Eddy Simulations) in which only the small eddies (fluctuations whose eddies are smaller than the computational cell) are modelled with a turbulence model. The LES equations read

$$\frac{\partial \bar{v}_i}{\partial t} + \frac{\partial \bar{v}_i \bar{v}_j}{\partial x_j} = -\frac{1}{\rho} \frac{\partial \bar{p}}{\partial x_i} + \nu \frac{\partial^2 \bar{v}_i}{\partial x_j \partial x_j} - \frac{\partial \tau_{ij}}{\partial x_j} = -\frac{1}{\rho} \frac{\partial \bar{p}}{\partial x_i} + \frac{\partial}{\partial x_j} \left((\nu + \nu_{sgs}) \frac{\partial \bar{v}_i}{\partial x_j} \right) \quad (3)$$

Note that the time dependence term (the first term on the left side) has been retained, because the large, time dependent turbulent (i.e. the resolved) fluctuations are part of \bar{v}_i and \bar{p} and are not modelled with the turbulence model. The term in front of the second equal sign includes the Reynolds stresses of the small eddies, which are called SGS (sub-grid stresses). This term must also – as in Eq. 2 – be modelled, and at the right side it has been modelled with a SGS turbulent viscosity, ν_{sgs} . The difference of ν_{sgs} compared to ν_t in Eq. 2 is that it includes only the effect of the *small* eddies. The ratio of ν_{sgs} to ν is of the order of 1 to 100. However, the ratio of the resolved to the modelled turbulence, $|\bar{v}'_i \bar{v}'_j| / |\tau_{ij}|$ (see Eqs. 2 and 3), is much larger than one. Hence, LES is much more accurate than RANS because only a small part of the turbulence is modelled with the turbulence SGS model whereas in RANS all turbulence is modelled. The disadvantage of LES is that it is *much* more expensive than RANS because a finer mesh must be used and because the equations are solved in four dimensions (time and three spatial directions) whereas RANS may be solved in steady state (no time dependence). When the flow near walls is of importance, it turns out that LES is prohibitively expensive because very fine cells must be used there. The reason is entirely due to physics: near the walls, the spatial scales of the “large” turbulent eddies which should be resolved by LES are in reality rather small. Furthermore, the “large” scales get smaller for increasing Reynolds number. Much research has the last ten years been carried out to circumvent this problem. All proposed methods combines RANS and LES where RANS is used near walls and LES is used away from the walls, see Fig. 1. These methods are called Detached Eddy Simulation (DES), hybrid LES/RANS or zonal LES/RANS. The focus of this report is zonal LES/RANS.

1.3 Zonal LES/RANS

Equations 2 and 3 can be written on a same form as

$$\frac{\partial \bar{v}_i}{\partial t} + \frac{\partial \bar{v}_i \bar{v}_j}{\partial x_j} = -\frac{1}{\rho} \frac{\partial \bar{p}}{\partial x_i} + \frac{\partial}{\partial x_j} \left((\nu + \nu_T) \frac{\partial \bar{v}_i}{\partial x_j} \right) \quad (4)$$

New SNIC Application System

A new application system was launched for the SNIC large scale application round this spring. The new system simplifies the application process for you in several ways. First, you get an overview of your past projects including project members and resource utilization. It also provides an easy way to include members from your old projects in your proposed project (but you can still add new members by providing their contact information). Among other neat features is the possibility for a principal investigator to add one of the co-investigators as a proxy, so that he or she can help fill in the application.

The new system is called SUPR, SNIC User and Project Repository. It is developed by a small team at the SNIC centers C3SE at Chalmers and NSC at Linköping University. The work is financed by SNIC and conducted under a steering committee with representatives from the Swedish National Allocations Committee, SNAC. The new system has advantages for SNAC too, such as providing a better overview during the entire review process and easier administration for reviewers and the SNAC working group.

Two-equation $k - \varepsilon$ Model

Near the walls, a RANS turbulence model is used for the turbulent viscosity, i.e. $\nu_T = \nu_t$ and away from the walls an LES turbulence model is employed, i.e. $\nu_T = \nu_{sgs}$. Note that the time dependence term is now retained also in the URANS region: near the wall we are using an *unsteady* RANS, i.e. URANS. Above, we have describe how to use the zonal LES/RANS method for flows near walls. Another form of zonal LES/RANS is *embedded* LES, in which an LES region is embedded in a URANS region. One example is prediction of aeroacoustic noise created by the turbulence around an external mirror on a vehicle [1]. The flow around the vehicle can be computed with RANS, but in order to predict the noise in the region of the external mirror we must predict the large, unsteady turbulent fluctuations and hence LES must be used in this region. In Section 4 we will present simulations using embedded LES in a simplified configuration represented by the flow in a channel in which RANS is used upstream of the interface and LES is used downstream of it, see Fig. 4.

2 The PANS $k - \varepsilon$ turbulence model

In the present work, the PANS $k - \varepsilon$ model is used to simulate wall-bounded flow at high Reynolds number as well as embedded LES. The turbulence model reads [2, 3] (here in a slightly simplified form to enhance readability)

$$\frac{\partial k}{\partial t} + \frac{\partial k \bar{v}_j}{\partial x_j} = \frac{\partial}{\partial x_j} \left[\left(\nu + \frac{\nu_T}{\sigma_k} \right) \frac{\partial k}{\partial x_j} \right] + P_k - \varepsilon \quad (5)$$

$$\frac{\partial \varepsilon}{\partial t} + \frac{\partial \varepsilon \bar{v}_j}{\partial x_j} = \frac{\partial}{\partial x_j} \left[\left(\nu + \frac{\nu_T}{\sigma_\varepsilon} \right) \frac{\partial \varepsilon}{\partial x_j} \right] + C_{\varepsilon 1} P_k \frac{\varepsilon}{k} - C_{\varepsilon 2}^* \frac{\varepsilon^2}{k} \quad (6)$$

$$C_{\varepsilon 2}^* = C_{\varepsilon 1} + f_k(C_{\varepsilon 2} - C_{\varepsilon 1}), \quad C_{\varepsilon 1} = 1.5, \quad C_{\varepsilon 2} = 1.9 \quad (7)$$

$$\nu_T = C_\mu \frac{k^2}{\varepsilon}, \quad C_\mu = 0.09 \quad (8)$$

Note that k and ε are always positive. The key elements in the present use of the PANS $k - \varepsilon$ model are highlighted in red. When f_k in Eq. 7 is equal to one, the model acts as a standard $k - \varepsilon$ RANS model giving a large turbulent viscosity. When f_k is decreased (to 0.4 in the present study), $C_{\varepsilon 2}^*$ in Eq. 7 decreases. As a result

- ε increases because the destruction term (last term in Eq. 6 which is the main sink term) in the ε equation decreases,
- k decreases because ε (last term in Eq. 5), which is the main sink term in the k equation, increases, and
- ν_T in Eq. 8 decreases because k decreases and ε increases.

Work is in progress to move the less extensive medium scale applications into SUPR too. The new features in the large scale system will be present here too, for example the overview of past projects and easy way to add members to a project. A new feature compared to the current system is that it will be possible to apply for resources at more than one SNIC center in one application. The new SUPR-based medium scale application system will be launched in the beginning of the summer when the large scale round is decided.

Hence, the turbulence model in Eqs. 5–8 acts as a RANS turbulence model (large turbulent viscosity) when $f_k = 1$ and it acts as an LES SGS turbulence model (small turbulent viscosity) when $f_k = 0.4$.

3 Zonal LES/RANS: wall modeling

3.1 The interface conditions

The interface plane (see Fig. 1) separates the URANS regions near the walls and the LES region in the core region. In the LES region $f_k = 0.4$ and in the URANS region $f_k = 1$. In the former region, the turbulent viscosity ν_T should be a small SGS viscosity and in the latter region it should be a large RANS viscosity. Hence ν_T must decrease rapidly when going from the URANS region to the LES region. This is achieved by setting the usual convection and diffusion fluxes of k at the interface to zero. New fluxes are introduced using smaller SGS values [4].

3.2 Results

Fully developed channel flow is computed for Reynolds numbers $Re_\tau = u_\tau \delta / \nu = 4000, 8000, 16000$ and 32000 ; the Reynolds number is varied by changing the viscosity, ν (u_τ and δ are set to one in all simulations). The baseline mesh has 64×64 cells in the streamwise (x) and spanwise (z) directions, respectively. Where should we locate the interface in Fig. 1? There are two main strategies, either to prescribe it manually or to do it automatically. In the latter case the ratio of the local cell size to the (modelled) eddy size is mostly used. This option is of course favored by the industry and it is used in all commercial codes. However, the automatic option seldom gives the optimal interface location. In the present study, we choose to set the location of the interface manually. The interface is set to $y^+ \simeq 500$ for all grids. $y^+ = u_\tau y / \nu$ is a non-dimensional wall distance. As mentioned above, $u_\tau = 1$ for all simulations and the Reynolds number is increased by decreasing the viscosity, ν . This means that the location of the interface moves closer to the wall when the Reynolds number is increased. The reason why we do this is related to the physics of near-wall turbulence mentioned in Section 1.2: the largest eddies near the wall (which in reality are rather small) and the region in which the wall has a strong effect on the fluid get smaller for increasing Reynolds number. The velocity profiles and the resolved shear stresses are presented in Fig. 2. As can be seen, the predicted velocity profiles are in good agreement with the log-law which represents

During the autumn we plan to extend the system with new functionality to further unify and simplify the administration for you as a user at one or more SNIC centers.

PETER MÜNGER

experiments. Figure 2b presents the resolved shear stresses. The interface is shown by thick dashed lines and as mentioned above it moves towards the wall for increasing Reynolds number. Outside the interface – in the LES region – the resolved fluctuations are large, and inside the interface – near the wall in the URANS region – the resolved fluctuations are reduced. The turbulent viscosity profiles are shown in Fig. 3 for three different resolutions in the $x - z$ plane. The turbulent viscosity is sharply reduced when going across the interface from the URANS region to the LES region and the resolved fluctuations (the Reynolds shear stress in Fig. 2b) increase. This shows that the model is switching from URANS mode to LES mode as it should. It is interesting to note that the turbulent viscosity in the LES region is not affected when the grid is refined (i.e. smaller cell size). Hence, the model yields *grid independent* results contrary to other LES/RANS models in which the SGS turbulent viscosity in the LES region always is related to the cell size. More detailed results can be found in [4].

4 Zonal LES/RANS: embedded LES

4.1 The interface conditions

The interface plane is now vertical, see Fig. 4. The interface conditions for k and ε are treated in the same way as in Section 3.1. The difference is now that “inlet” turbulent fluctuations must be added to the LES \bar{v}_i equations (Eq. 3) to trigger the flow into turbulence-resolving mode. Anisotropic synthetic turbulent fluctuations are used [5, 6].

4.2 Results

The Reynolds number for the channel flow, see Fig. 4, is $Re_\tau = 950$. Figure 5a presents the mean velocity and the resolved shear stresses at three streamwise locations, $x = 0.19, 1.25$ and 3 (recall that the interface is located at $x = 1$). At $x = 3$, the predicted velocity agrees very well with the experimental log-law profile. The resolved streamwise velocity fluctuations are zero in the URANS region, as they should (Fig. 5b), and they increase sharply over the interface thanks to the imposed synthetic turbulent “inlet” fluctuations. The turbulent viscosity is reduced at the interface from its peak RANS value of approximately 80 to a small LES value of approximately one (these values are both fairly low because of the low Reynolds number). Hence, it is seen that the present model successfully switches from URANS to LES across the interface. The results will be presented in more detail in [4].

LARS DAVIDSON

References

- [1] J. Ask and L. Davidson. Flow and dipole source evaluation of a generic SUV. *Journal of Fluids Engineering*, 132(051111), 2010.
- [2] S. S. Girmaji. Partially-Averaged Navier-Stokes model for turbulence: A Reynolds-averaged Navier-Stokes to direct numerical simulation bridging method. *Journal of Fluids Engineering*, 73(2):413–421, 2006.
- [3] J. Ma, S.-H. Peng, L. Davidson, and F. Wang. A low Reynolds number variant of Partially-Averaged Navier-Stokes model for turbulence. *International Journal of Heat and Fluid Flow*, 32:652–669, 2011. 10.1016/j.ijheatfluidflow.2011.02.001.
- [4] L. Davidson. A new approach of zonal hybrid RANS-LES based on a twoequation model (submitted). In *ETMM9: International ERCOFTAC Symposium on Turbulence Modelling and Measurements*, Thessaloniki, Greece, 2012.
- [5] L. Davidson. Using isotropic synthetic fluctuations as inlet boundary conditions for unsteady simulations. *Advances and Applications in Fluid Mechanics*, 1(1):1–35, 2007.
- [6] L. Davidson and S.-H. Peng. Embedded LES with PANS. In *6th AIAA Theoretical Fluid Mechanics Conference, AIAA paper 2011-3108*, 27-30 June, Honolulu, Hawaii, 2011.

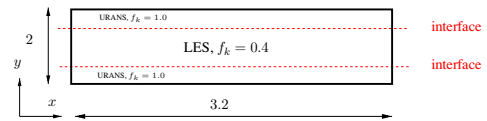


Figure 1: The LES and URANS regions. Fully developed channel flow. Periodic boundary conditions are applied at the left and right boundaries.

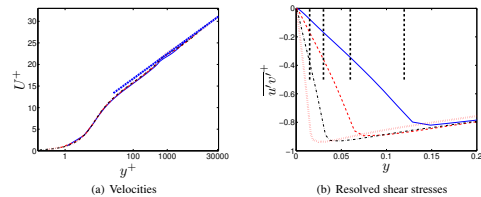


Figure 2: Velocities and resolved shear stresses. $(N_x \times N_z) = (64 \times 64)$: —: $Re_\tau = 4000$; - - -: $Re_\tau = 8000$; ···: $Re_\tau = 16000$; |||: $Re_\tau = 32000$.

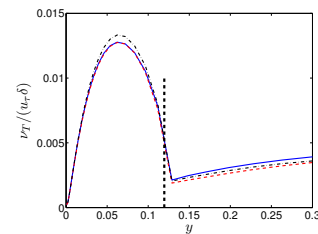


Figure 3: Turbulent viscosity. $Re_\tau = 4000$. —: $(N_x \times N_z) = (64 \times 64)$; - - -: $(N_x \times N_z) = (32 \times 32)$; ···: $(N_x \times N_z) = (128 \times 128)$

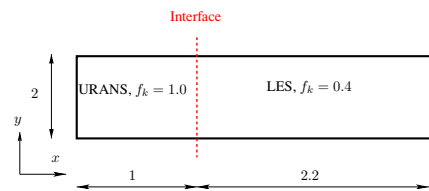


Figure 4: The LES and URANS regions. The left boundary is an inlet and the right boundary is an outlet.

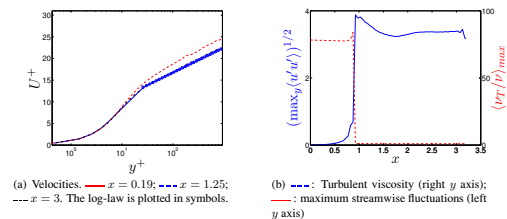


Figure 5: Channel flow with inlet and outlet. (a) Velocities; (b) maximum resolved streamwise turbulent fluctuations and turbulent viscosity versus x .

Lars Davidson was appointed to professor at Chalmers in 1995. His research topic is CFD and turbulence modelling. Since 1995 he is the head of the Division of Fluid Dynamics at the Department of Applied Mechanics.





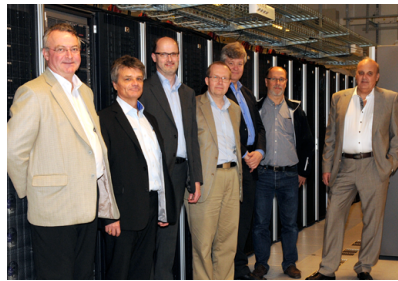
Three New Supercomputers to NSC

NSC has signed a contract with Go Virtual Nordic AB of delivery of three new computer systems from HP. The largest system, Triolith, consists of 1200 compute servers and will have a max performance of 338 Teraflops (at nominal clock frequency). Triolith is funded by The Science Council through SNIC and will become a generally available SNIC resource. The second system, Krypton, is funded by SMHI and will be used for weather model development and climate research. Krypton consists of 240 compute servers. The third system with 72 compute servers is named Skywalker and will be located at Saab for their use.

To get an early start, we have chosen to stage the delivery and installation. In May, 20 percent of Triolith (240 compute servers), 40 percent of Krypton (96 servers) and 100 percent of Skywalker is installed at NSC. Our plan is to make

them available for users in July. The second stage, including the remaining parts of the hardware, will be installed after the summer. To prepare for the installation, we will need to shut down a large part (up to fifty percent) of Neolith. We will need users' assistance to transfer parts of Neolith's workload onto Triolith as soon as we have it ready for production.

NICLAS ANDERSSON, NSC



Hardware facts

All three clusters are based on HP's modular chassis, ProLiant SL6500, equipped with eight SL230s Gen8 servers. In each server there are two Intel Xeon E5-2660 (2.2 GHz) processors. Each processor has AVX, 20 MB L2-cache, PCIe 3.0, and four memory channels equipped with DDR3-1600 modules.

In Triolith, 1144 of the servers are equipped with 32 Gigabyte of memory and 56 with 128 Gigabyte of memory, in total 42.75 Terabyte primary memory. Total theoretical performance at nominal clock frequency is 338 Teraflops. For Krypton and Skywalker, the corresponding performance is 67.6 and 20.3 Teraflops respectively.

All servers are interconnected with FDR Infiniband (56 Gigabit/s) from Mellanox in a fat-tree topology with a 2:1 fan-out. For disk storage the clusters will be connected to existing storage equipment.

Ivar Ekström, Sales, Go Virtua, Kent-Roger Wistrand, Country Manager, HP, Niclas Andersson, Technical director, NSC, Bengt Persson, Director, NSC, Kenneth Benedictsson, Sales, HP, Hans Rickardt, support specialist, HP and Jan Wallenberg, CEO, Go Virtual, visit the main NSC computer room in connection with signing the contract.

Intel HPC Training at NSC Continues

On March 20–22, NSC hosted a follow-up on last year's popular Intel HPC training event. This time the Intel expert, Heinrich Bockhorst, gave a three-day in-depth training on the Intel Trace Analyzer and Collector (ITAC) tool. ITAC, which is Intel's derivative of the well-known Vampir tool, can be used to visualize and understand parallel application behavior, evaluate profiling statistics, analyze performance, and learn about communication patterns etc.

Sixteen HPC users from both industry and academia participated in the training class that was held in a lecture room at Linköping University, Campus Valla in house Galaxen, which is also the

building that houses the NSC offices. The Kappa system at NSC was used for the hands-on exercises that were a significant part of the training class.

The training received overall very good feedback from the participants and NSC hopes to be able to welcome you to participate in another focused Intel training already later this year. Keep a lookout for an invitation on our web site or in your mailbox.

NSC would like to thank Intel and especially the instructor, Heinrich Bockhorst, for a very educational and successful event.

TORBEN RASMUSSEN



Heinrich Bockhorst is working as a technical consulting engineer for high performance computing in Europe. He is member of the developer products division (DPD) within the Software & Services Group. Currently his work is focused on many core enabling and very high scaling hybrid programming targeting Top30 accounts. He is conducting 3-4 customer trainings on Cluster Tools per year and he is now in charge of developing new training material for Europe.



National Supercomputer Centre, Linköpings universitet, 581 83 Linköping, Sweden
Tel: +46 (0) 13-28 26 18, fax: +46 (0) 13-28 25 35, e-mail: info@nsc.liu.se
www.nsc.liu.se